

The ATLAS Pixel Detector operation and performance

A. Andreazza^{*†}

INFN Sezione di Milano and Dipartimento di Fisica, Università di Milano, Via Celoria 16, I-20133, Milano, Italy

E-mail: Attilio.Andreazza@mi.infn.it

The ATLAS Pixel Detector is the innermost detector of the ATLAS experiment at the Large Hadron Collider at CERN. It consists of 1744 silicon sensors equipped with approximately 80×10^6 electronic channels, providing typically three measurement points with high resolution for particles emerging from the beam-interaction region. The complete Pixel Detector has been taking part in cosmic-ray data-taking since 2008. Since November 2009 it has been operated with LHC colliding beams at $\sqrt{s} = 900$ GeV, 2.36 TeV and 7 TeV.

The detector operated with an active fraction of 97.2% at a threshold of 3500 e , showing a noise occupancy rate better than 10^{-9} hit/pixel/BC and a track association efficiency of 99%.

The Lorentz angle for electrons in silicon is measured to be $\theta_L = 12.11^\circ \pm 0.09^\circ$ and its temperature dependence has been verified. The pulse height information from the time-over-threshold technique allows an improvement of the point resolution using charge sharing and particle identification at low momentum using the specific energy loss.

19th International Workshop on Vertex Detectors - VERTEX 2010

June 06 - 11, 2010

Loch Lomond, Scotland, UK

^{*}Speaker.

[†]for the ATLAS Collaboration

1. Introduction

ATLAS [1] is a general purpose particle physics experiment at the Large Hadron Collider at CERN. The Pixel Detector [2] is the innermost component of its tracking systems, consisting of hybrid silicon pixels. The Pixel Detector started operation in 2008 with cosmic-ray data-taking and took part in the 2009 and 2010 LHC runs. This paper describes the detector operation in the LHC collisions at $\sqrt{s} = 7$ TeV, starting from the hardware detector calibration in section 3, continuing with the operation with LHC beams and offline calibration in section 4 and providing a summary of the performance in section 5.

2. The ATLAS Pixel Detector

The ATLAS Pixel Detector is made of three barrel layers (with radii 50.5 mm, 88.5 mm and 122.5 mm and 800 mm length) and two end-caps, each one constituted of three disks (located at 495 mm, 580 mm and 650 mm from the detector centre). It provides three precision measurement points for tracks with pseudorapidity $|\eta| < 2.5$. The detector layout is shown in figure 1.

The basic components of the detector are the modules, that are identical for barrel and disks. In the barrel they are arranged in overlapping staves of 13 modules each, while in the disks they form 6-modules sectors, for a total of 1744 modules. Each module contains 47232 silicon pixels resulting in a total of more than 80×10^6 pixels covering a surface of 1.7 m². All components are designed to sustain the radiation dose of 500 kGy, which is expected during the detector lifetime. The detector structure is made of low-mass carbon fibres and integrates the cooling system, resulting in a total contribution to the radiation length of about 3% per layer. Resolutions better than 10 μm for 50 μm pitch in the azimuthal direction (local- x) and 115 μm for 400 μm pitch along the beam direction (local- y) have been measured in test beams [5].

Each module is composed of a sensor, 16 front-end (FE) chips and a flex hybrid containing control and transmission electronics [2].

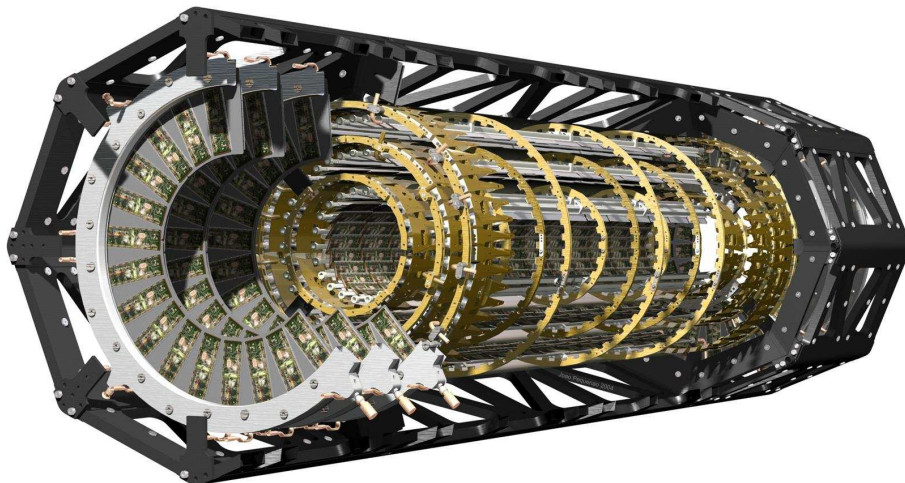


Figure 1: Schematic view of the ATLAS Pixel Detector.

The FE chips are bump-bonded to the pixels using solder or indium bump bonds with a $50\ \mu\text{m}$ pitch. Each chip contains 18 columns times 160 rows of readout cells, realized with 250 nm CMOS technology. The FEs provide threshold adjustment and charge measurement using the time-over-threshold (ToT) of the output signal [3]. The sensor is made of n^+ -in- n silicon with a typical pixel size of $50 \times 400\ \mu\text{m}^2$ (with the short side along the $R\Phi$ direction). To avoid dead regions, some pixels with modified geometries (*long* and *ganged* pixels) are present close to the borders of the FE. The measured sensor thickness is $256 \pm 3\ \mu\text{m}$. A flexible kapton circuit, wire-bonded to the FEs and glued on the reverse side of the sensor, provides a bias voltage of 150 V. It contains the Module Controller Chip (MCC) that controls the FE and has basic event reconstruction capability. The MCC and FE clock is given by the LHC 25 ns bunch crossing (BC) interval.

The readout system uses optical transmission for the outgoing module data and the incoming timing, trigger and control data. The transmission is based on VCSELs operating at a wavelength of 850 nm and radiation-hard fibres [4].

During the ATLAS data-taking period in 2010, 46 out of 1744 modules are not active, 18 due to missing bias connections and 28 because of faulty data and control connections. In addition a few FEs are found to be defective. The resulting active fraction of the detector is 97.2%. Most of the temporary faults during operation are due to failures of the optical transmitter on the off-detector readout electronics, which can be promptly replaced, and do not result in significant losses of data.

3. Detector calibration

The calibration of the Pixel Detector is a multi-step process. First the optical data and control links are set to optimal parameters; secondly the front-end electronics is tuned to provide uniform thresholds and response to injected charge.

Threshold calibration of the front-end electronics is performed by injecting signals of known amplitude into the input of the electronics chain. The fraction of observed hits as a function of the injected charge is fitted with an error function, providing the threshold, defined as the 50% efficiency point, and the electronic noise, as the Gaussian width parameter of the error function. Figure 2 shows the threshold and noise distributions for the nominal working point with a threshold of 4000 e . Channels can be individually tuned using a 7-bit DAC with a uniformity of 40 e RMS. In these conditions the average noise level is 160 e for most pixels, and slightly higher for long and ganged pixels: 185 e and 280 e , respectively. Similar performance is achieved with the 3500 e threshold settings used for the 2010 data-taking period.

The ToT measurement is adjusted using a 3-bit DAC, to provide a value of 30 BC for an input charge of 20000 e , corresponding to the most probable signal generated by a minimum ionizing particle. A calibration of the ToT-to-charge relationship is afterwards performed varying the injected charge. The relationship is almost linear and the measurement has a resolution of approximately 1 BC at ToT = 30 BC, corresponding to a charge resolution of approximately 660 e . An example of calibration curve is shown in figure 3.

A final calibration step is detector timing [6]. In the initial LHC runs, the low trigger rate and long bunch separation allows the readout of multiple consecutive BCs. The distribution of hits across BCs can be used to improve the detector timing relative to the corrections computed from

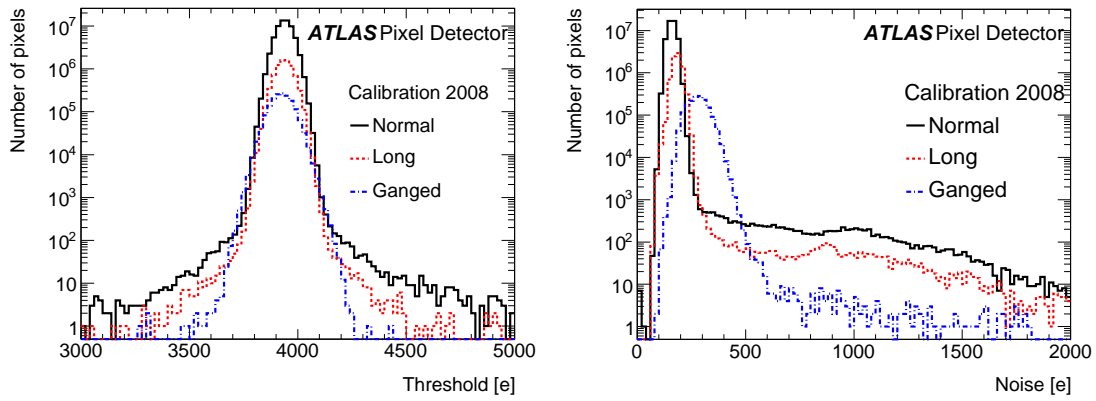


Figure 2: Pixel Detector threshold (left) and noise (right) distributions from calibrations based on charge injection.

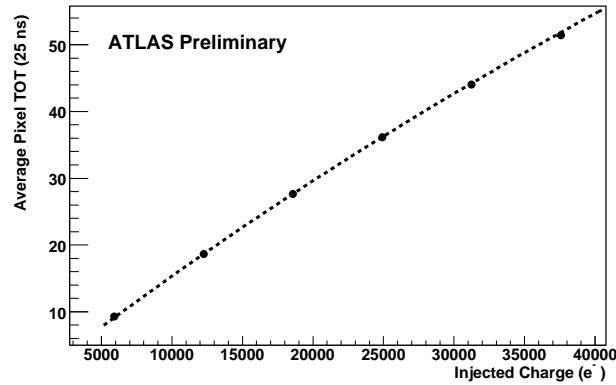


Figure 3: Average ToT value as a function of the collected charge for one FE chip. The dashed line is the curve used to calibrate the charge versus ToT relationship.

measured signal delays in the cables and in the readout electronics. After this timing adjustment, more than 99.9% of the pixel clusters are collected in a single BC.

4. Operation with beams

The operation of the detector with LHC beams aims to meet two major requirements: detector safety and high data-taking efficiency. The former requirement imposes to keep the sensor bias voltage switched off when LHC beams are not stable, and to ramp it up only when the beams are in their stable colliding position.

To increase the data-taking efficiency, a *warm start* procedure has been devised to accelerate the begin of data-taking after the ramp-up. It consists of configuring the FE electronics and starting data-taking even during the initial beam operation by the LHC, but with all channels disabled in the readout, in order not to flood the DAQ system with noise hits from the undepleted detector.

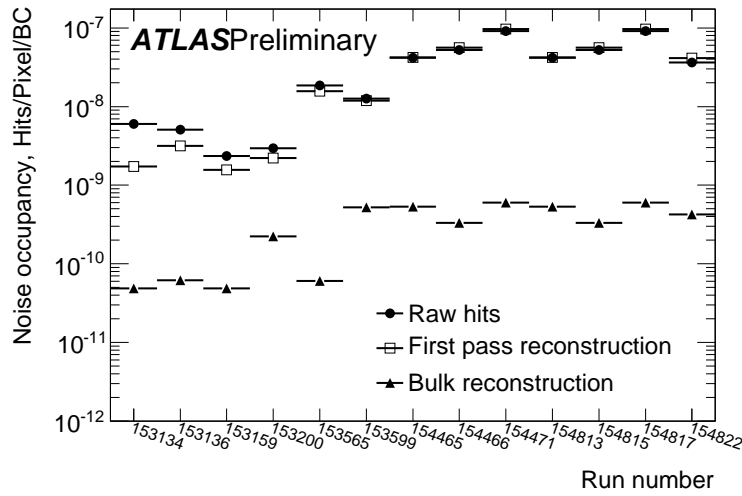


Figure 4: Pixel Detector noise rate from raw data, after the first pass of reconstruction (without offline noise masks) and after the bulk reconstruction using the offline noise mask.

As soon as the sensor bias is turned on, data-taking can start just after enabling all the readout channels. This procedure requires a few minutes and has a minimal impact on the overall ATLAS up-time.

The Pixel Detector DAQ has also the capability to automatically remove noisy modules whose large amount of data is slowing the acquisition rate. These modules are subsequently automatically reinserted into the detector readout if their noise rate falls down to an acceptable level.

The data quality is assessed online, sampling events at each level of the ATLAS trigger system. Occupancy, readout errors and ToT are monitored internally in the off-detector electronics after level-1 and level-2 triggers. Detailed cluster properties are then extracted and track reconstruction is performed on events passing the last trigger level (Event Filter).

The offline calibration algorithms, used to provide the best possible data quality for subsequent physics analysis, form an important aspect of the detector operation. They consist of a noise suppression procedure and the calibration of the charge interpolation algorithm. The calibration procedures are performed on special samples of events immediately after each data-taking run and the results is applied to the subsequent bulk data reconstruction, which is delayed by 36 hours in order to collect the outcome of the calibration procedures from all ATLAS sub-detectors.

The noise rate is dominated by a few hundred pixels. For this reason, the noise is reduced either by excluding pixels from readout (*online* mask) or by not using them in data reconstruction (*offline* mask). The online mask is provided for each readout configuration, while the offline mask is computed on a calibration sample provided by triggering on empty bunch crossings. Pixels are considered noisy if they have an occupancy larger than 10^{-5} hits per BC. In figure 4, the noise occupancy is shown for some data-taking runs during 7 TeV collisions. Raw data are compared to first pass reconstruction data (before noise mask computation) and to the bulk reconstruction: the occupancy is less than 10^{-9} hits per pixel per BC.

The spatial resolution depends on the readout tuning, on the cluster size and on the particle

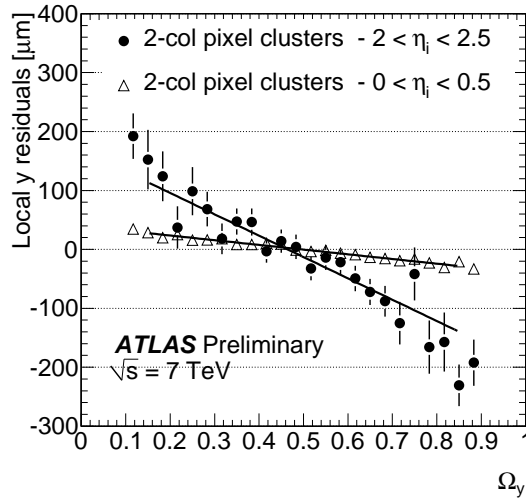


Figure 5: Pixel Detector residuals in the local- y coordinate as a function of the charge sharing Ω for 2-column clusters in different pseudorapidity regions.

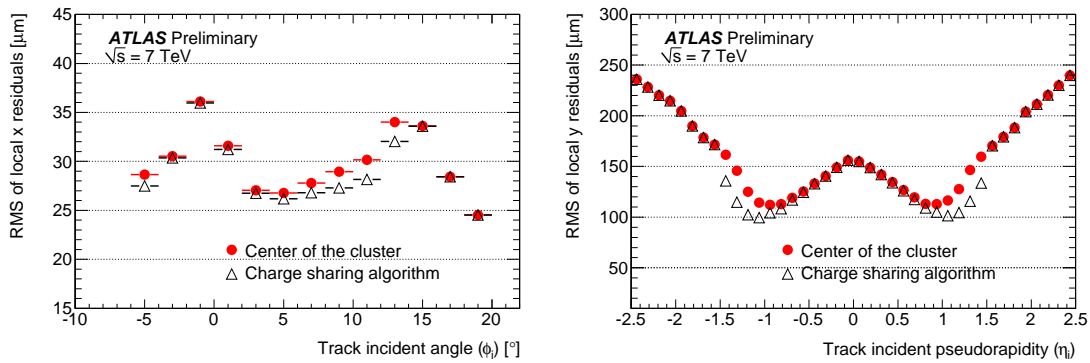


Figure 6: RMS of the residual distributions for cluster local- x as a function of the track incident angle (left) and cluster local- y as a function of track pseudorapidity (right).

incident angle. It is improved by adding a correction term proportional to *charge sharing* to the geometrical centre of the cluster. The charge sharing variable, Ω , is defined as the ratio between the charge collected in the first pixel of the cluster and the sum of charges collected in both the first and last pixels. The weight for the correction is fit from data for different cluster sizes and ranges of incident angle [8]. As an example, figure 5 shows, for 2-pixel wide clusters in the local- y direction, the average value of the residuals between the centre of the cluster position and the track extrapolation as a function of the Ω variable. Due to the high statistics needed for this calibration method, it is performed only before a major data reprocessing.

5. Detector Performance

The intrinsic hit efficiency was measured in cosmic-ray events by extrapolating tracks through

the detector and counting the numbers of measurements on a track and of *holes*, where a hit would be expected but is not found. The measured hit efficiency was $(99.974 \pm 0.004(\text{stat.}) \pm 0.003(\text{syst.}))\%$ for the barrel part, if non-operational modules are excluded [7]. A more relevant quantity for tracking performance is the *association efficiency*, the probability to associate a Pixel Detector hit to a track. This takes into account the fact that existing clusters may be rejected during track reconstruction because of ambiguities in their assignment to tracks or because their residual gives a too big contribution to the track fit χ^2 . This efficiency is about 99% for most layers. Only the outermost disks have a 1–2% lower efficiency due to few regions of disconnected bump bonds. Overall the biggest source of inefficiency are the 46 inactive modules that correspond to 2.64% of the detector (see section 2).

The values of RMS of the residuals with respect to the track extrapolation for the local- x and local- y position of the clusters, as a function of the track incident angle and pseudorapidity, are shown in figure 6. The improvement due to the charge sharing correction obtained from the calibration procedure in section 4 is clearly visible. The residual distribution width is determined both by the track extrapolation uncertainty and the finite detector resolution, the former being the dominant contribution for the Pixel Detector.

ATLAS uses a 2 T solenoidal magnetic field to measure the momentum of particles in the inner tracker. The field causes charge carriers inside the Pixel Detector sensor to drift towards the electrodes forming an angle with respect to the normal to the module surface, the *Lorentz angle*, θ_L . When estimating the particle crossing point, this angle should be subtracted from the incident angle of particles [5]. The distribution of the cluster size as a function of the particle incident angle is used to measure the Lorentz angle, which corresponds to the minimum of this distribution. The average cluster size, projected on the local- x direction ranges from 1.4 at this minimum up 2.4 for high momentum tracks. A full study of the systematic uncertainties was performed on cosmic-ray data [7], giving a value of $\theta_L = 11.77^\circ \pm 0.03^\circ \pm_{0.23^\circ}^{0.13^\circ}$ at -3°C and a temperature dependence of $d\theta_L/dT = (-0.042 \pm 0.003)^\circ/\text{K}$. With collision data, both at centre-of-mass energies of 900 GeV and 7 TeV, the measurement is less accurate, due to the smaller range of particle incident angles (figure 7). The mean temperature of the detector is lower, giving a larger measured value of $12.1^\circ \pm 0.09^\circ$ for a threshold of 3500 e .

The specific energy loss, dE/dx , associated to particles is measured from the charge collected in the clusters, after a selection that excludes regions where the charge collection efficiency is poor. The track dE/dx is defined as the truncated average of the energy deposition of each individual cluster, by removing the one with the highest collected charge, in order to reduce the Landau tails. A relative resolution of 12% is measured for particles with $p > 3$ GeV and at least 3 clusters per track. The dependence of dE/dx on the track momentum and charge is displayed in figure 8. Separate bands for π^\pm , K^\pm and $p(\bar{p})$ are identified. For positive charges also the band corresponding to deuterons is visible.

6. Conclusions

The ATLAS Pixel Detector has been operated successfully during the LHC 2010 run at a centre-of-mass energy of 7 TeV, with a fraction of 97.2% of the detector being operational. Data-taking and calibration procedures have been developed to guarantee a safe data-taking with a high

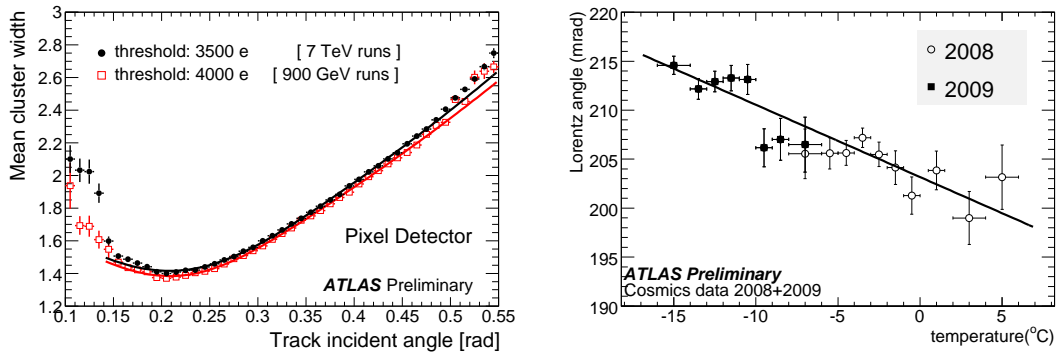


Figure 7: Lorentz angle measurements: (left) cluster size as function of the track incident angle for data at $\sqrt{s} = 900$ GeV and 7 TeV, (right) value of θ_L measured on cosmic-ray data as a function of the module temperature.

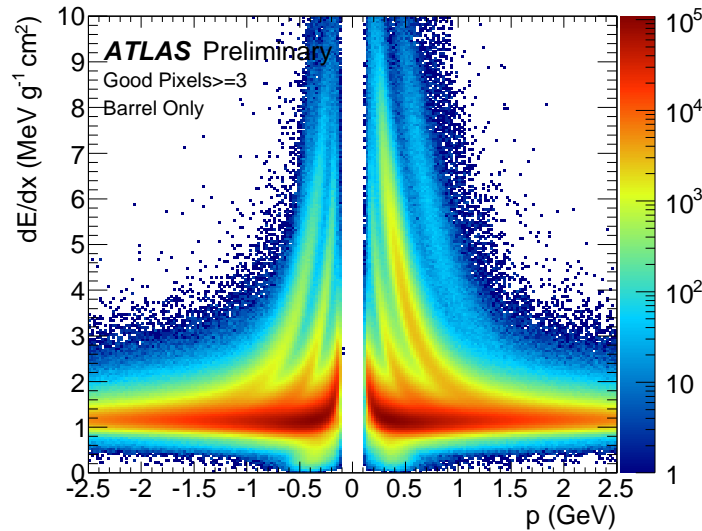


Figure 8: dE/dx measurement in the Pixel Detector as a function of $Q \times p$ for particles with at least three associated hits.

fraction of up-time. Online and offline data quality monitoring and calibration procedures are used to provide high-quality data for track reconstruction.

A random noise occupancy of 10^{-9} hit/pixel/BC has been measured after masking a few hundreds noisy pixels out of a total of 80×10^6 channels. The track association efficiency is 99% for most of the detector.

The Lorentz angle for electrons in a 2 T magnetic field has been measured to be $12.11^\circ \pm 0.09^\circ$ at 12°C (statistical error only), in agreement with previous measurements with cosmic-ray data and their temperature dependence.

The collected charge is measured with the time-over-threshold technique and has been used to improve the detector resolution with respect to a simple binary readout and to provide a dE/dx

measurement with a 12% resolution, allowing particle identification at low momenta.

References

- [1] The ATLAS Collaboration, G. Aad et al., *The ATLAS Experiment at the CERN Large Hadron Collider*, JINST **3** (2008) S08003
- [2] G. Aad et al., *ATLAS pixel detector electronics and sensors*, JINST **3** (2008) P07007
- [3] I. Peric et al., *The FEI3 readout chip for the ATLAS pixel detector*, Nucl. Instrum. and Methods **A565** (2006), 178-187
- [4] K. K. Gan et al., *Optical Link of the ATLAS Pixel Detector*, Nucl. Instrum. and Methods **A570** (2006), 292-294
- [5] I. Gorelov et al., *A measurement of Lorentz angle and spatial resolution of radiation hard silicon pixel sensors*, Nucl. Instrum. and Methods **A481** (2002), 204-221
- [6] I. Ibragimov, *Timing Behavior of the ATLAS Pixel Detector in Calibration, Cosmic-Ray and Collision Data*, these proceedings
- [7] The ATLAS collaboration, G. Aad et al., *The ATLAS Inner Detector commissioning and calibration*, arXiv:1004.5293, to be published on Eur. Phys. J. C
- [8] S. Montesano, *Commissioning of the tracking system in the ATLAS detector*, Ph.D. Thesis, Università degli Studi di Milano, Milano, 2010, CERN-THESIS-2010-018